Molecular Crystals and Liquid Crystals
Publication details, including instructions for authors and subscription information:
http://www.tandfonline.com/loi/gmcl16

Disclinations and Properties of the Directorfield in Nematic and Cholesteric Liquid Crystals

Alfred Saupe [a]
[a] Liquid Crystal Institute Kent State University, Kent, Ohio, 44242
Version of record first published: 21 Mar 2007.

To cite this article: Alfred Saupe (1973): Disclinations and Properties of the Directorfield in Nematic and Cholesteric Liquid Crystals, Molecular Crystals and Liquid Crystals, 21:3-4, 211-238

To link to this article: http://dx.doi.org/10.1080/15421407308083320

Molecular Crystals and Liquid Crystals. 1973. Vol. 21, pp. 211–238

Printed in Great Britain

Disclinations and Properties of the Directorfield in Nematic and Cholesteric Liquid Crystals†

ALFRED SAUPE

Liquid Crystal Institute
Kent State University
Kent, Ohio 44242

Received February 8, 1973

Abstract—Structure and properties of disclination lines and disclination points in nematic and cholesteric liquid crystals are reviewed. An equivalence between the directorfield of nematics and electrostatic or magnetostatic fields in two-dimensions is pointed out.

Disclination lines can be classified in singular and non-singular lines. Disclination points correspond always to singular solutions. They are often associated with non-singular lines. Experimental observations of disclinations, of surface patterns in cholesterics, and of cholesteric textures are described. Structural features of special cholesteric " focal-conic " and " fan " texture are discussed in terms of the vectorfield defined by the twist axis.

The well-known characteristic feature of nematic liquid crystals is threadlike structures that can be observed with a polarizing microscope. The name " nematic " appropriately stresses this feature. It is derived from the Greek word for thread.

The first steps to the interpretation of the threads as disclinations of the directorfield have been made by Oseen.[1–4] Newer research started with Frank[5] who derived Oseen's theory of curvature elasticity on a more general basis and presented it in a simpler form.

The state of a cholesteric liquid crystal is similar to that of nematics described by a directorfield. One should expect accordingly that both kinds of liquid crystals form similar disclinations or threads. However, the observed optical textures and frameworks of disclinations are very different due to differences in interactions and stability of the disclinations. We consider first the case of nematic liquid crystals and summarize some basic theoretical results.

† Plenary Lecture presented at the Fourth International Liquid Crystal Conference, Kent State University, August 21–25, 1972.

1. Torque Density in the Rotation Invariant Approximation

In the most simple case the torque density in the directorfield of nematics and cholesterics can be written:

$$\tau = 2k_2 \mathbf{L} \times \operatorname{curl} \mathbf{L} + k\mathbf{L} \times \nabla^2 \mathbf{L} \tag{1}$$

It is assumed here that the three elastic constants for splay, twist and bend are all equal. **L** is a unit vector parallel to the preferred orientation or to the local optical axis. **L** and $-\mathbf{L}$ have the same physical meaning. The director is in general a continuous function in space except along certain lines or points where it changes discontinuously. The assumption of equal deformation constants is especially convenient for nematics for which $k_2 = 0$. In that case τ is invariant with respect to a rotation of **L**. This approximation is therefore sometimes called the isotropic case. In the rotation invariant approximation singular solutions for the directorfield can easily be obtained explicitly. They are useful for the following qualitative considerations. In real cases the elastic constants differ from one another and the structures of the disclinations are accordingly more complicated.[6,7]

2. Singular Solutions in Planar Nematic Textures, and Schlierentextures with Vertical Threads

In an ideal planar texture all field lines of the directorfield run parallel to a fixed plane. Planar textures are often realized to a good approximation in thin films. They correspond to equilibrium structures and are usually assumed when surface conditions permit it. Deviations from planarity occur then only along the disclinations. We use in the following the term planar texture in general for fields which can be considered as planar outside the surroundings of disclinations.

Let us first consider an ideal planar texture. We close the z-axis perpendicular to the field and can write

$$\mathbf{L} = \cos\phi, \sin\phi, 0 \tag{2}$$

For $\tau = 0$ the angular variable ϕ has to be a solution of the Laplace equation

$$\Delta\phi = 0 \tag{3}$$

In cases where ϕ is a function of two coordinates only, the solutions are harmonic functions. The often-discussed singular solutions of interest[1-7] for nematics with vertical threads are

$$\phi_p = s\alpha_p + \phi_{op};\ s = \pm\tfrac{1}{2},\ \pm 1,\ \pm\tfrac{3}{2}\ldots i\alpha_p;\ = \tan^{-1}\frac{y-y_p}{x-x_p} \tag{4}$$

The singularity is positioned at x_p, y_p and ϕ_{op} is an additive constant.

There is another mathematical approach for planar structures with **L** dependent on x and y only. It correlates the directorfield directly to electro- and magnetostatic fields in two dimensions and to the potential flow of incompressible liquids.

We can set

$$\mathbf{L} = \frac{\operatorname{grad} u}{|\operatorname{grad} u|} \tag{5}$$

where u is again a solution of the 2-dimensional Laplace equation. The general solution is an analytical function $\omega = u + iv$. We can choose $\mathbf{L} \| \operatorname{grad} u$ and the field lines are then given by the curves $v = \text{const}$. It is obvious now that 2-dimensional electro- or magnetostatic field in the vacuum and the potential flow fields can also be interpreted as directorfields. It should be noticed, however, that the directorfield contains additional singularities at the points where $|\operatorname{grad} u| = 0$.

The considered singular solutions are now given by

$$\omega_p = \exp(-i\phi_{op})(z-z_p)^{1-s};\ s = \pm\tfrac{1}{2},\ -1,\ \pm\tfrac{3}{2}\ldots \tag{6}$$

The case $s = 1$ appears as a special case:

$$\omega_p = \exp(-i\phi_{op}) \log(z-z_p) \text{ for } s = +1 \tag{7}$$

Figure 1 represents the familiar structures of the singularities. When ϕ_{op} is varied the singularities are rotated by a corresponding amount with the exception of the $+1$ singularity which changes its structure from radial straight lines to logarithmic spirals and finally concentric circles. The lines for $s = +\frac{1}{2}$ are confocal parabolas, for $s = -1$ equilateral hyperbolas.

We obtain a general solution for the considered planar case by superposition of such singularities. The resulting texture corresponds to the experimentally observable Schlierentextures with point-like singularities or, more correctly, with vertical threads.

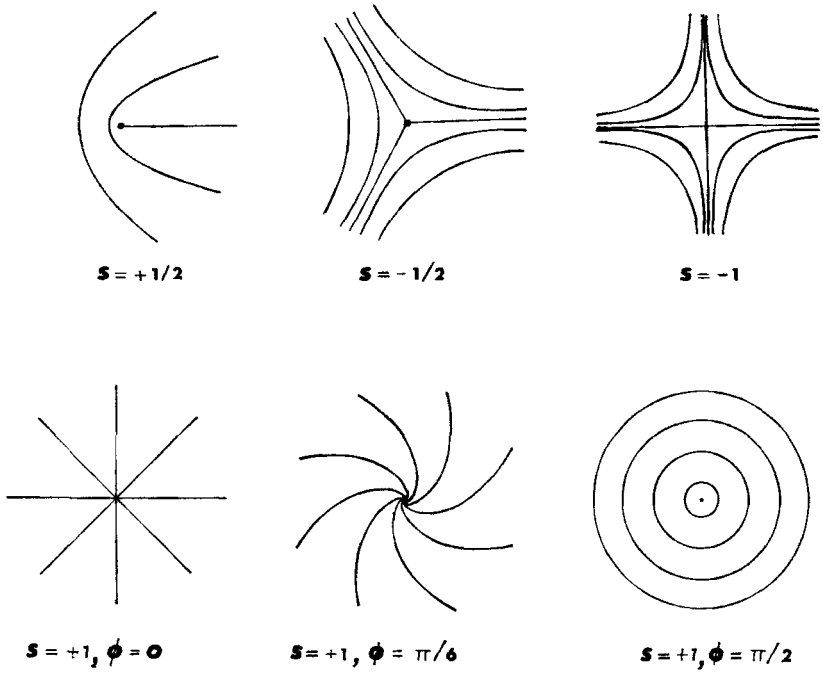

Figure 1. Directorfield of vertical threads in planar textures, 2-dimensional approximation. ($\phi = \phi_{op}$ of Eqs. 4, 5 and 6).

The disappearance of τ is not sufficient for a static equilibrium. The deformation energy depends on the distance between disclinations and accordingly disclinations interact with each other. The forces are similar to the magnetic interactions between currents. The interaction between the vertical threads p and q at $\mathbf{r}_p$ and $\mathbf{r}_q$ is given[7,8] by Eq. (8)

$$\mathbf{F}_{pq} = -2\pi k s_p s_q \frac{\mathbf{r}_{pq}}{r_{pq}^2} \tag{8}$$

Here $\mathbf{F}_{pq}$ is the force per unit length acting on the thread at $\mathbf{r}_p$ and $\mathbf{r}_{pq} = \mathbf{r}_p - \mathbf{r}_q$. Disclinations of opposite sign attract each other. They can merge and disappear or form a new disclination with a characteristic number equal to the sum of s of the merging threads.

3. The Core Structure of Disclinations

A problem which has attracted much attention is the core structure of disclinations. Are they singular also in the 3-dimensional approach? The case $s = +1$ has been carefully studied recently.[9–13]

For a discussion of the core structures we have to use a 3-dimensional approach and look for solutions which can be fitted together with the planar structure outside the cores.

We write now

$$\mathbf{L} = \sin\theta\cos\phi, \sin\theta\sin\phi, \cos\theta \tag{9}$$

and use cylinder coordinates $x = r\cos\alpha$, $y = r\sin\alpha$, z. A set of suitable solutions can be obtained with

$$\phi = s\alpha + \phi_0\,;\; s = \pm 1,\ \pm 2, \ldots \tag{10}$$

and $\theta = \theta(r)$ as a solution of the differential equation

$$\frac{\partial^2\theta}{\partial r^2} + \frac{1}{r}\frac{\partial\theta}{\partial r} - \frac{s^2}{r^2}\cos\theta\sin\theta = 0 \tag{11}$$

Equation (11) is easily integrated. It gives in general an elliptical integral. We are interested in the solutions with $\theta = 0$ for $r = 0$ and $\theta = \pi/2$ for $r = r_{\pi/2}$ when $r_{\pi/2}$ denotes the core radius. These solutions are:

$$\tan\frac{\theta}{2} = (r/r_{\pi/2})^{|s|} \tag{12}$$

The energy density in the core of whole numbered lines (s integer) remains according to this result finite. These lines do not correspond to singular solutions of the directorfield. The solution $s = +1$ and $\phi_0 = 0$ may be realized in a capillary[9,11] (Fig. 2a).

It is interesting to study also the hypothetical case that **L** rotates by π between capillary wall and center (Fig. 2b). One finds that there is no finite equilibrium value for $r_{\pi/2}$, the distance for the 90° turn. It goes to zero and accordingly the energy density in the center to infinity. This structure is therefore not stable. It would lead to a rupture along the center line and finally a uniform parallel alignment would result.

Schematic structures of $+1$ vertical threads in Schlierentextures are shown in Fig. 3. When the Schlierentexture is due to the

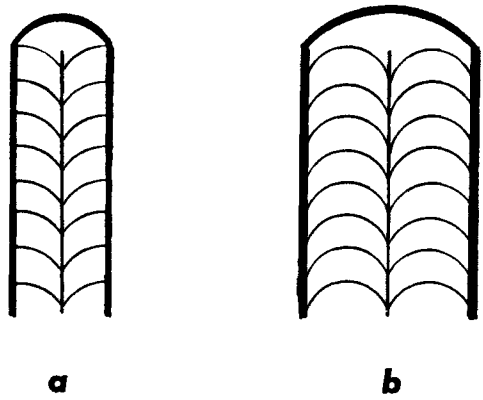

Figure 2. Directorfield in capillaries, axial sections: (a) normal surface orientation with a $\pi/2$ rotation between wall and center, $+1$, 0 disclination; (b) parallel surface orientation with a π rotation between wall and center, instable structure.

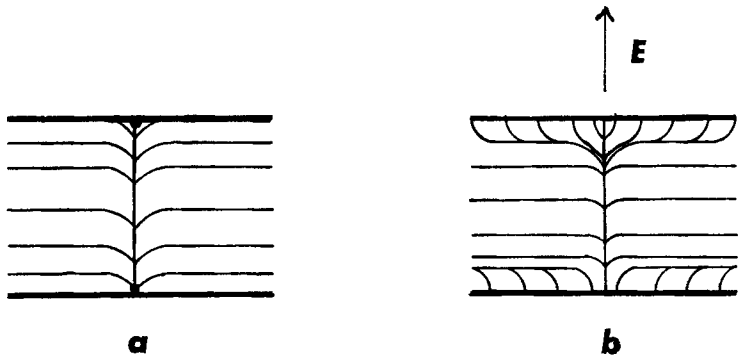

Figure 3. Sections through vertical threads in Schlierentexture: (a) thread ending in singular points; (b) field-induced thread without singularities.

boundary conditions the threads may end in singular points. It is also possible to induce a Schlierentexture with vertical threads by an electric field acting on a pseudoisotropic film. The dielectric anisotropy has to be negative and the field must be applied normal to the film. The threads end now without singularities.

Figure 4 gives an example for a field-induced Schlierentexture. Only $+1$ and -1 vertical lines are formed. The picture is taken with monochromatic light. When the applied field is relatively low a nice interference pattern is obtained which allows us to recog-

nize directly the sign of the singularity. The pattern has cylindrical symmetry for $s = 1$ and a 4-fold symmetry axis for $s = -1$. The lines interact in the same way as in normal Schlierentextures.

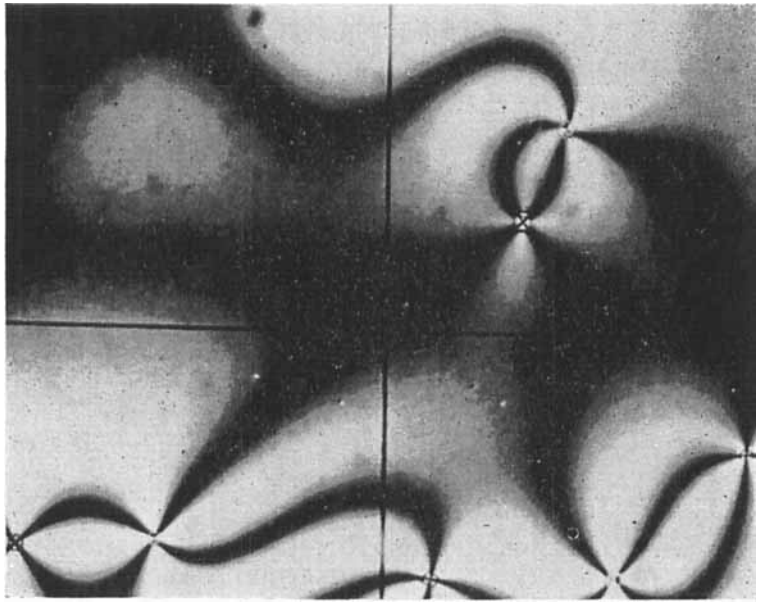

Figure 4. Electric field-induced Schlierentexture. MBBA (N-(*p*-methoxybenzylidene)-*p*-*n*-butylaniline) at 20°C, crossed polarizers, approx. 26 ×. Film *ca.* 70 μm thick, field applied vertical, 6 V rms, 300 Hz.

4. Solutions for Singular Points

Let us consider now the singular points associated with $+1$ and -1 lines in more detail. In the rotation invariant approach the solution for the main point singularities that occur in nematics can be readily obtained. We set again

$$\mathbf{L} = \sin\theta\cos\phi, \sin\theta\sin\phi, \cos\theta \tag{13}$$

and use spherical coordinates $x = \rho \sin\delta\cos\alpha$, $y = \rho\sin\delta\sin\alpha$, $z = \rho\cos\delta$.

$$\phi = s\alpha + \phi_o\,;\; s = \pm 1,\ \pm 2, \ldots \tag{13a}$$

θ is obtained from the differential equation

$$\sin^2 \delta \frac{\partial^2 \theta}{\partial \delta^2} + \sin \delta \cos \theta \frac{\partial \theta}{\partial \delta} - s^2 \sin \theta \cos \theta = 0 \tag{14}$$

We find selecting the solutions with $\theta \to \delta$ for $s \to 0$

$$\tan \theta/2 = (\tan \delta/2)^{|s|} \tag{15}$$

For the singular structures of interest we have $s = \pm 1$ and therefore $\theta = \delta$.

Figure 5 presents the structures of some singular points. The

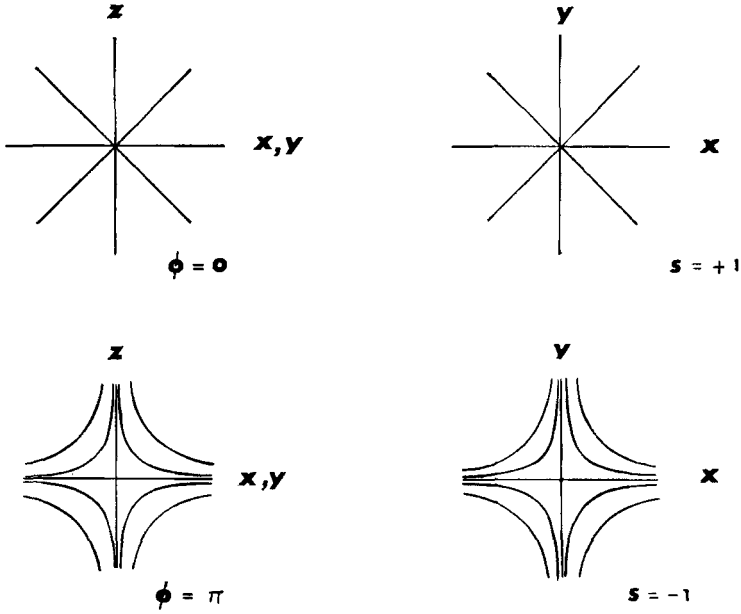

Figure 5. Directorfield of singular points. ($\phi \equiv \phi_0$ of Eq. 13a)†.

sections through the x, y and the x, z and y, z planes give fields which are identical with the structures of the $+1$ and -1 singularities in two dimensions (Fig. 1). Any field on the left hand side of the figure may be combined with anyone on the right hand side to give a possible point singularity. We will accordingly in the following characterize the main types of singular points by the numbers (ϕ_o, s).

† Note added in proof: Dr. J. Nehring brought to my attention that the values of ϕ_0 are interchanged ($\phi_0' = \phi_0 + \pi$) when the solutions of (14) with $\theta \to \pi - \delta$ for $\rho \to 0$ are selected.

5. Experimental Examples for Singular Points in Nematics

It is easily possible to produce singular points experimentally by choosing the boundary conditions suitably. Figure 6a shows the field that may be present in a capillary when **L** is perpendicular oriented all along the surface. The liquid will have to form then at least one singular point. Singular points in capillaries were first described by Williams *et al.*[9] In general, there will be an odd number of singular points present or other singular structures that replace the points.

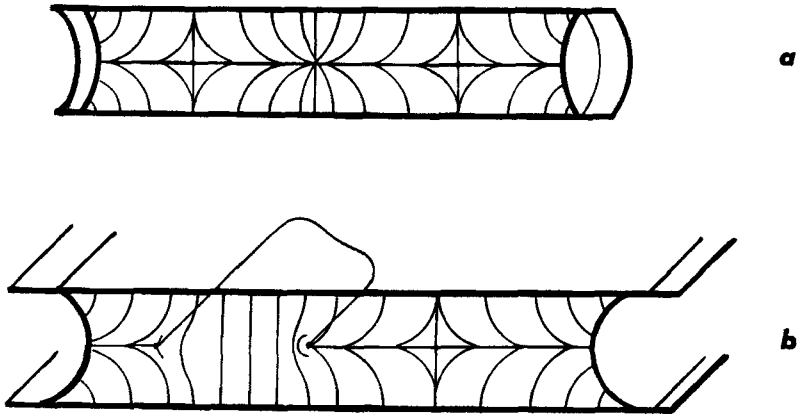

Figure 6. (a) Point singularities in a capillary. The points are arranged along the center and alternate between type π, 1 and 0, 1; (b) Simplified director-field in a plane film with perpendicular surface orientation. Section through horizontal singular loop and a singular point.

Figure 6b illustrates the vectorfield of a plane layer with the same boundary conditions. When the inner area has a pseudoisotropic texture, we can expect a $\frac{1}{2}$ line along the interface liquid-air (see Fig. 9). Horizontal lines in films with planar textures and uniform boundary conditions always separate areas which differ in the number of rotations that **L** makes along a vertical line through the film. The difference in rotations between areas separated by a thread is equal to 2π times the characteristic number of the thread. In films with vertical surface orientation, one can also observe point singularities of the types $s = +1$ and $s = -1$. They usually form after a

disturbance in the areas with a π rotation. In capillaries only $s = +1$ points will normally form.

Figures 7 and 8 show microphotographs of singularities in a capillary filled with MBBA after a surface treatment with lecithin. The capillary has a diameter of about 1 mm. Figure 8 shows a loop that has formed instead of a 0, +1 point. The loop remains unchanged until it finally merges with a π, +1 point and disappears. No 0, +1 points could be observed in these rather thick capillaries. They were always replaced by loops. The microphotographs (Figs. 9–11) show singularities in a pseudoisotropic film of MBBA sandwiched between glass plates. Figure 11a–b demonstrates the attraction between points of opposite s-values. The two points merge and disappear finally.

6. Topological Considerations to the $\frac{1}{2}$ Lines

The +1 and −1 singularities of Oseen and Frank correspond to singular points in the 3-dimensional generalization. A simple geometrical consideration shows that the 2-dimensional $\frac{1}{2}$ points correspond in three dimensions to singular lines.

In ideal planar structures the disclination lines can be characterized by $|s|$ the number of 2π turns that **L** makes along a closed curve around the thread. (The sign of s is no characteristic feature for curved lines since their structure varies with the orientation of the line axis). In the non-ideal, real cases the same procedure is useful but the curve has to be kept in the planar part of the directorfield. For the general 3-dimensional case we have to modify the procedure. We again consider the orientational change of **L** along a closed curve. Each orientation of **L** can be presented by a point on a unit sphere. The orientations of **L** along the curve in the directorfield are accordingly represented by a curve on the unit sphere. For a closed curve in the field (primary curve) two essentially different cases are possible:

1) the assigned curve is also closed,
2) the assigned curve ends on the opposite point of the sphere, $\mathbf{L} \rightarrow -\mathbf{L}$.

In the first case it may be possible to contract the curve in the field steadily to a point so that at the same time the corresponding curve

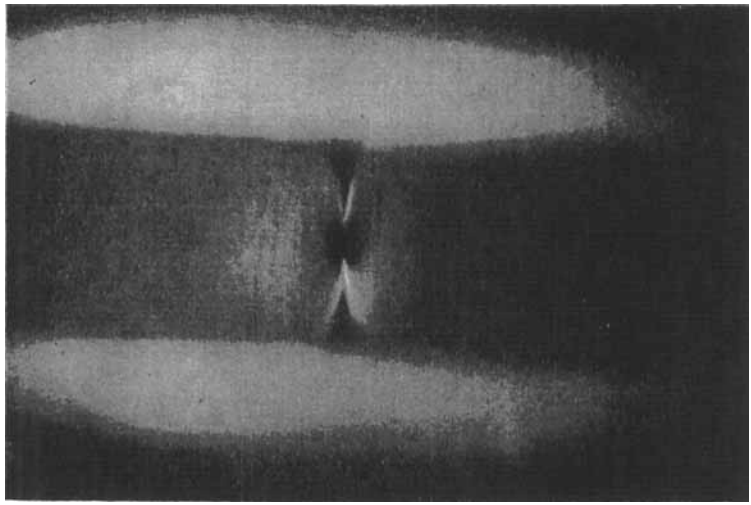

Figure 7. Singular point (π, $+1$) in capillary; unpolarized light, approx. 53 ×.

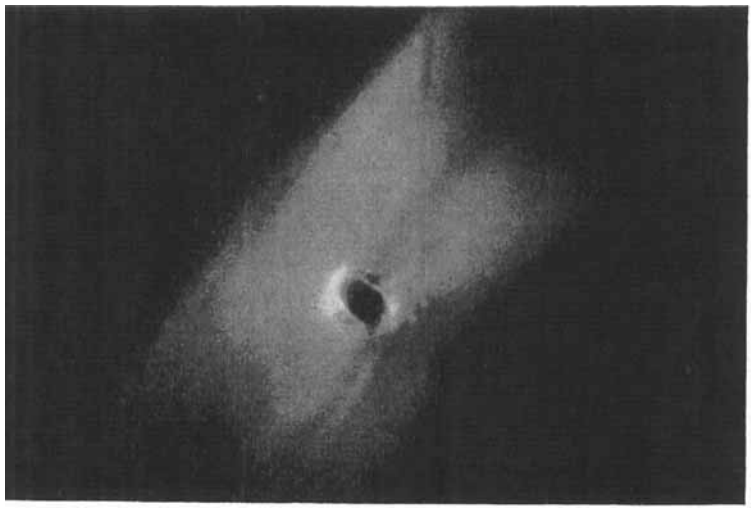

Figure 8. Disclination loop in capillary; crossed polarizers, approx. 32 ×.

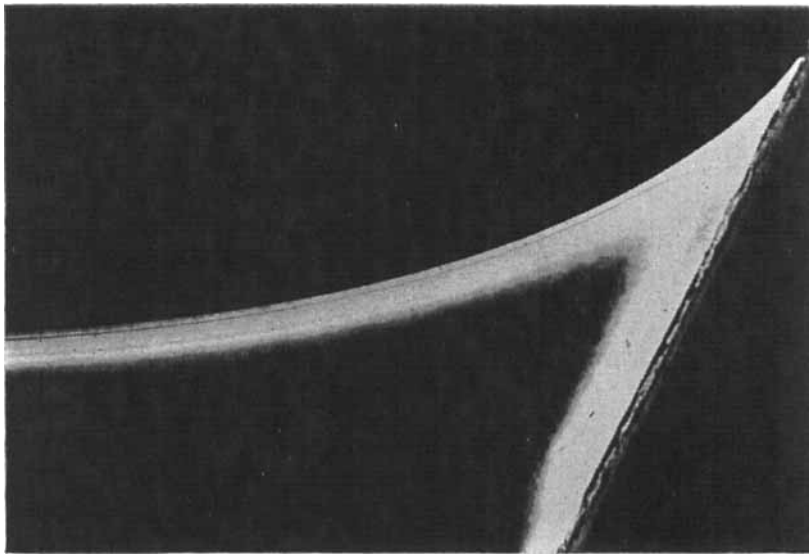

Figure 9. Singular line ($-\frac{1}{2}$) along interface nematic liquid-air; in pseudo-isotropic film, *ca.* 70 μm thick. Crossed polarizers approx. 58 $\times$. The line ends at Teflon spacer on the right side.

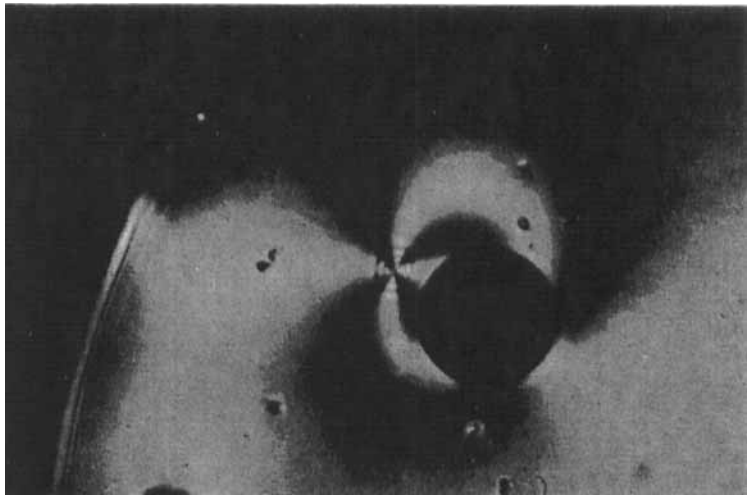

Figure 10. Singular point (0, -1) near air bubble in disturbed area of a pseudoisotropic film, *ca.* 70 μm thick. Crossed polarizers, approx. 175 $\times$.

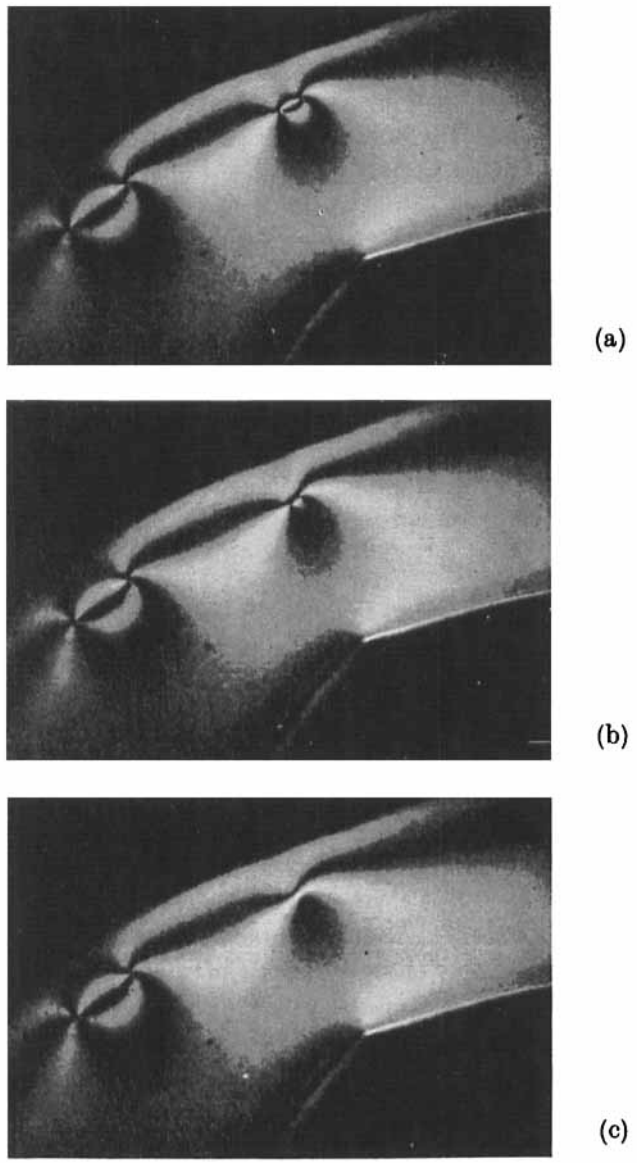

Figure 11. Pairs of singular points in disturbed area of a pseudoisotropic film; crossed polarizers, approx. 22 ×. The sequence demonstrates attraction and merging of singular points.

on the sphere contracts steadily to a point. It means that the primary curve did not include a singular line.

In the second case it is not possible that the curve on the sphere contracts steadily to a point, because the end point can only come back discontinuously to the starting point. Any simply connected surface which lays completely in the liquid crystal and has such a primary curve as a boundary must therefore contain a singularity.

It follows that Frank–Oseen's $\frac{1}{2}$ points correspond in fact to cuts through singular lines. These lines can never end in the liquid crystal. They must either form closed loops or end on the surface. Even in case they lead to a particle or an air bubble floating in the liquid crystal, another line must start from there. Analogous considerations for planar textures show that $|s| = 1$ lines form either closed loops or end on surfaces or at $\frac{1}{2}$ lines. This follows since for planar textures the number of rotations of **L** along a closed curve can change only discontinuously.

7. Structural Features of Cholesteric Liquid Crystals

The characteristic feature by which cholesteric liquid crystals differ from nematics is the spontaneous formation of twisted structures. It reflects the existence of a preferred screw sense in the molecular geometry. Accordingly, we have now in general $k_2 \neq 0$ and corresponding changes in interactions and stabilities of disclination lines. The lines no more merge and cancel each other as in nematics and complicated stable networks of disclination lines may form (Fig. 12). The "streaks" in planar cholesteric films that often form a crackle consist of bundles of thin individual lines. A single line itself may show a number of complicated features. Such features have been studied recently in cholesterics with a weak twist ($p = 10$–$100\ \mu$) by Rault.[14–16]

A useful structural concept was introduced by Kleman and Friedel.[17] It allows us to visualize and describe the structure of special disclinations in cholesterics by relatively simple pictures. Kleman and Friedel postulate a quasi-layered structure and thus explicitly take into account the natural twist of these systems. Instead of using the concept of a layered structure to account for the twist, we may also consider the field of the twist axis (t) in

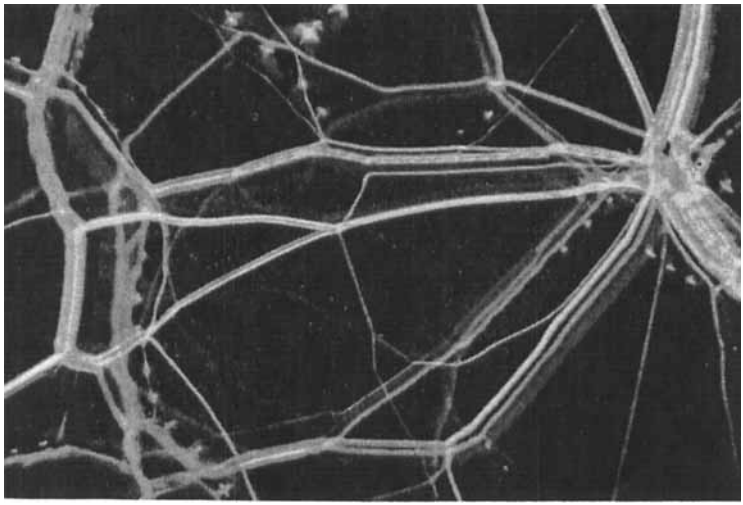

Figure 12. Disclinations in MBBA + 10% ChN at 20°C; darkfield, crossed polarizers, approx. 53 ×, focused on inner part of film. (ChN, Cholesteryl-nonanoate. Concentrations are estimates).

addition to the directorfield. The two concepts are essentially equivalent with the " twistfield " being identical with the vectorfield defined by the normals to the " layers ".

The twistfield accordingly suffices the condition $\mathbf{t} \cdot \operatorname{curl} \mathbf{t} = 0$ which means that in this field no twist deformations are allowed. The concept of " layers " or of a twistfield is an approximation which for the core of disclinations may not be valid or useful. We assume that the core structures are similar to structures that may be found in nematics. This is, of course, especially true for cholesterics with a weak twist.

8. Horizontal Lines in Planar Textures

In an ideal planar texture the twist is uniform and the twist axis field consists of straight lines which in thin films are often perpendicular to the plane of the film. The directorfield is thus given by Eq. (2) with $\phi = (2\pi/p)z$ where p is the pitch of the helical structure and the z axis $\| \mathbf{t}$.

The most simple type of disclinations is " horizontal " lines, that is lines which are parallel to the surfaces of constant **L** in planar

textures. They are formed in wedge-shaped samples when the surface orientation is fixed, and are known as Grandjean steps.

Figure 13 shows the structure of Grandjean lines as proposed by Kleman and Friedel.[17] The lines can be interpreted as a combination of a pair $+\frac{1}{2}$ and $-\frac{1}{2}$ lines in the field of the twist axis (indicated

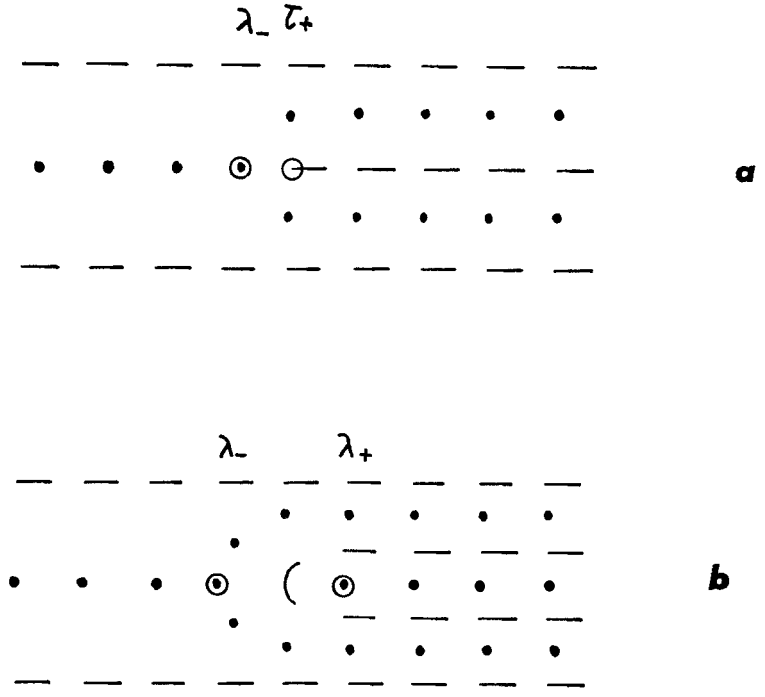

Figure 13. Vertical sections through horizontal lines.[17] The orientation of the director is indicated by lines (**L** in plane of drawing) and by points (**L** vertical): (a) disclination line with $s = \frac{1}{2}$; (b) disclination line with $s = 1$.

by circles in Fig. 13). The latter lines are denoted[17] by $\lambda+$ and $\lambda-$ or $\tau+$ and $\tau-$. In the center of λ-lines **L** is parallel to the line axis. The τ-lines correspond to true singular lines in the directorfield. The orientation of **L** is not defined along the line axis in this case.

The horizontal or Grandjean lines in planar cholesteric films, similar to horizontal lines in nematics, separate areas which differ in the number of (helical) turns of **L**. The difference measured in 2π turns is again equal to the earlier introduced characteristic number

s of the disclination line. It is a function of the separation of the pair.

Grandjean lines have been extensively studied. Theoretical estimations for the energy have been made by Kleman and Friedel[17] and based on de Gennes' model for the line by Scheffer.[18] Recently also, experimental methods have been used for an estimation of their energy.[14,19]

9. Vertical Lines in Planar Textures

Another case of special interest is vertical lines. They can be represented in two equivalent pictures. Figure 14 shows schematic structures for $\frac{1}{2}$ lines. The structure on the left-hand side is obtained by continuously twisting a nematic parallel to the axis of the line. The directorfield is accordingly given by Eq. (2) with $\phi = s\alpha + 2\pi z/p$. A surface $\mathbf{L} = \text{const.}$ of the resulting structure ($\alpha = (\phi_o - 2\pi z/p)/s$)

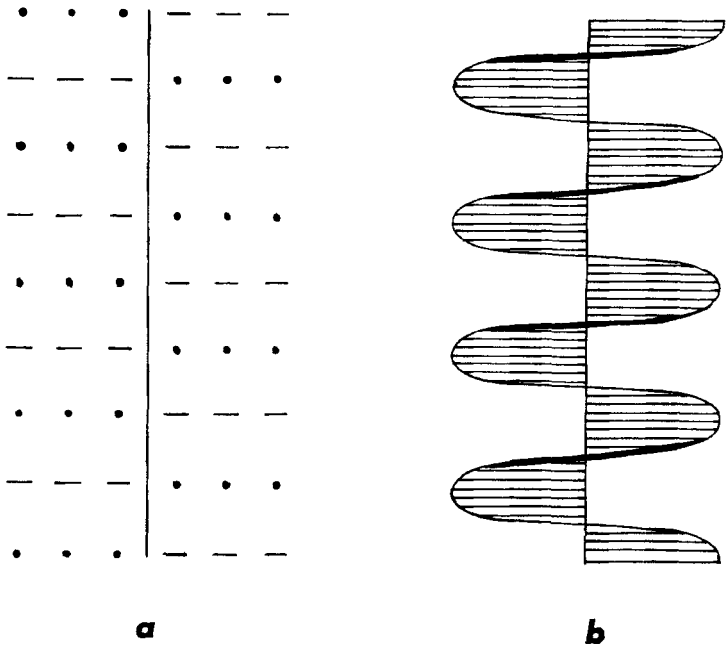

Figure 14. Section through vertical lines parallel to line axis, $s = -\frac{1}{2}$: (a) orientation of $\mathbf{L}$; (b) surface $\mathbf{L} = \text{const.}$

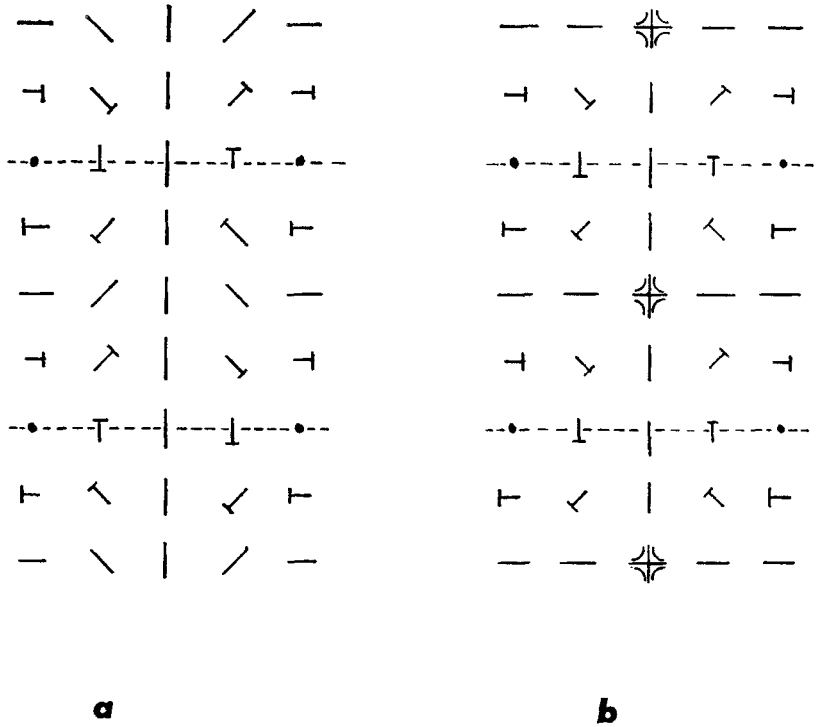

Figure 15. Sections through vertical lines (+1) indicating core structures: (a) continuous structure; (b) structure with (π, 1) points. Shorter lines with a dash mark inclined positions of L. The screw sense of the structure along the two dashed lines is opposite in (a) but equal in (b).

is indicated on the right side. It forms a screw and explains why vertical lines can also be regarded as screw dislocations.[20]

The core of a +1 vertical line in cholesterics presents some unexpected features. When we take the solution for a continuous core as in nematics and subject it to the twist, we obtain a core structure as shown in Fig. 15a. It is also continuous but not stable because it contains regions which are twisted in the wrong sense. The requirement of a uniform screw sense leads to a core that combines a series of point singularities type ($\pi + 1$,) with a distance equal to $p/2$ (Fig. 15b). Such a string of point singularities with a distance $p/2$ are in fact often found in isolated vertical +1 lines.[14,16] Occasionally the singular point may be replaced by a circular narrow loop of a $\frac{1}{2}$ line.

10. Oblique Lines in Planar Textures

Lines that transmit a planar texture under an oblique angle usually form curled curves possibly with equidistant inversion points. Figure 16 shows an example of a curled line. We assume as for vertical lines that the directorfield in the horizontal planes is essentially the same as that of a planar nematic ($\phi = \alpha s + \phi_0$ outside the core). For $s = +1$ oblique lines form curled curves with inversion points separated by a vertical distance equal to $p/2$.[14] They

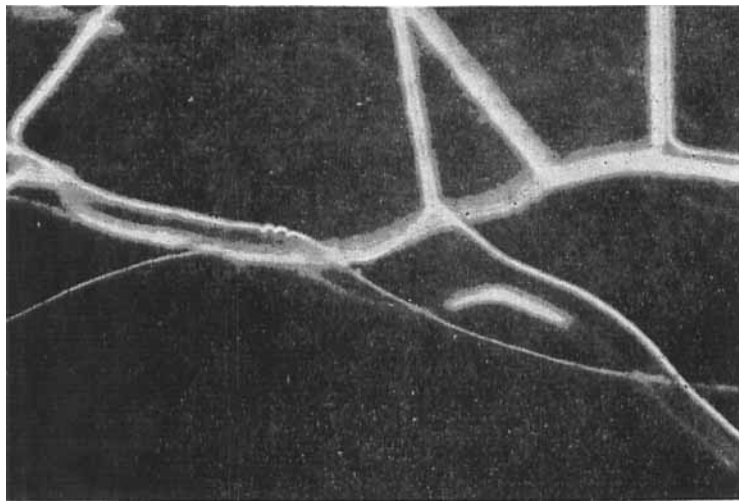

Figure 16. MBBA + 4% ChN at 20 °C; darkfield, without analyzer, approx. 175 ×, focused on interior part. Disclinations are horizontal with the exception of the curled section.

correspond to the series of singular points in vertical lines. In other cases when the core in the corresponding vertical lines is uniform we may qualitatively explain the formation of curled lines as follows. The energy of the oblique lines depends on two angles:

1) angle between line axis and vertical,
2) angle between the horizontal projection of the line axis and a symmetry axis of directorfield (outside the core).

When the coupling between the latter two directions is strong the horizontal component of the axis will follow the twist and a smooth

curled curve may form. On the other hand, when the coupling is weak, the component will follow the twist only to a certain degree and then reverse, possibly connected with the formation of a sharp bend. A more complicated behavior can be observed for $s = -1$ lines. They may form a combination of vertical sections and curved horizontal lines.[14,16]

11. Surface Patterns of Disclinations

In case of special boundary conditions, for instance, with approximately perpendicular orientation regular patterns of disclination lines can be observed which develop just below the surface. The twisted structure of the bulk material cannot readily adapt to this boundary condition and for this reason a network of lines may form

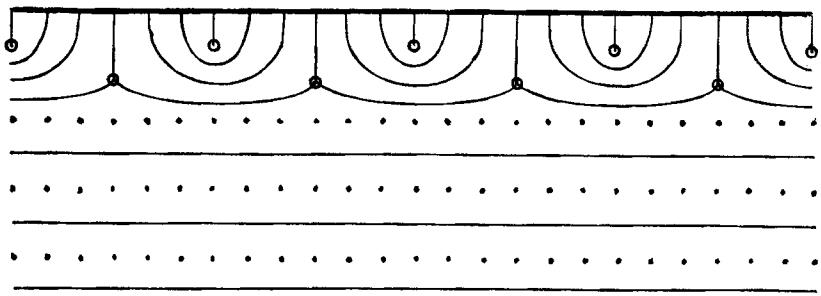

Figure 17. Vertical section through twisted planar texture. An alternating series of $+\frac{1}{2}$ and $-\frac{1}{2}$ singular lines provides adaption to perpendicular surface orientation.

which covers the whole surface. To illustrate this point let us consider a surface with perpendicular orientation that covers a planar twisted texture. The liquid could adapt to this condition by developing a series of $+\frac{1}{2}$ and $-\frac{1}{2}$ lines as indicated in Fig. 17. There are other solutions to this problem and the structure of actual surface lines will certainly be different. Other factors could also contribute to their formations. Figures 18 to 22 show some of the surface patterns that can be observed in MBBA and cholesteryl nonanoate (ChN) mixtures.

Figures 18 and 19 present pictures of small droplets. The dark field observation (Fig. 19) shows clearly the disclination line that

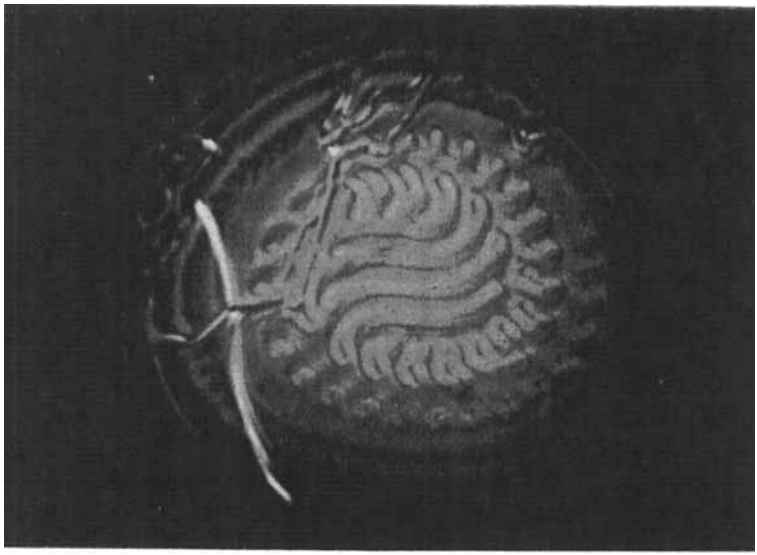

Figure 18. Uncovered droplet. MBBA + 10% ChN, at 20°C; crossed polarizers, approx. 640 ×.

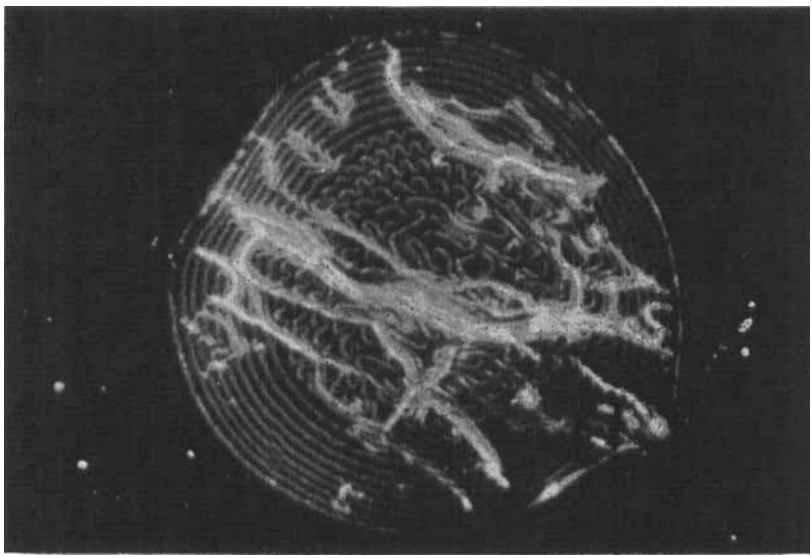

Figure 19. Uncovered droplet. MBBA + 10% ChN at 20°C; darkfield, approx. 240 ×.

winds along below the surface. Near to the edge the line runs approximately parallel to the boundary and produces the appearance of a step droplet. The brighter disclination lines in Fig. 19 lay to their major part deeper in the liquid.

Figure 20a shows part of the surface pattern of a larger droplet.

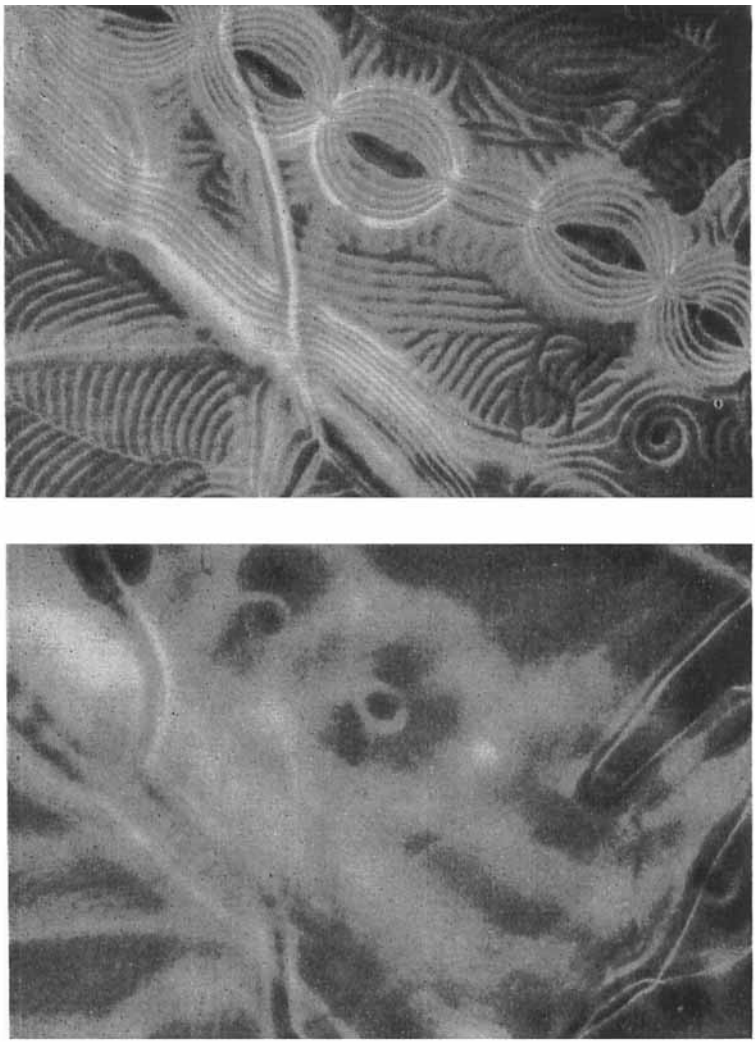

Figure 20. MBBA + 10% ChN at 20 °C; partial darkfield, approx. 175 ×: (a) focused on free surface; (b) focused on (lower) glass liquid interface.

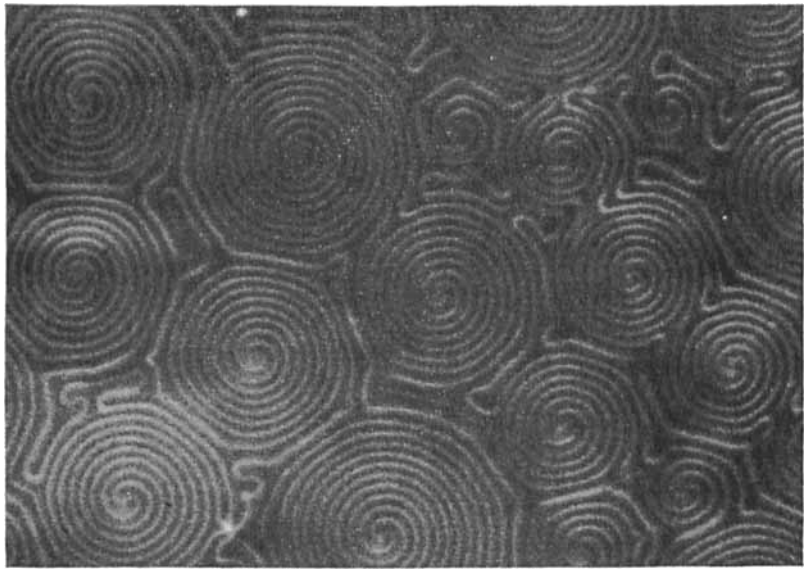

Figure 21. Free surface, MBBA + 10% ChN at 20 °C; darkfield, approx. 450 ×, monochrom. light.

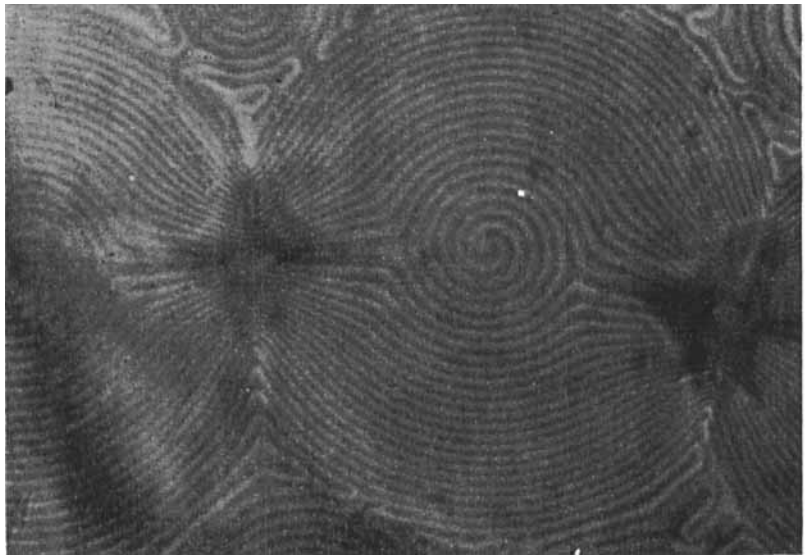

Figure 22. Free surface, MBBA + 10% ChN at 20 °C; darkfield, approx. 640 ×, monochrom. light.

Characteristic features are beat-like patterns that arrange to strings, and spirals. When focused deeper below the surface, these patterns disappear and the usual disclination lines are visible (Fig. 20b).

In larger droplets the spirals were the most stable surface pattern. Fresh samples show a more or less irregular, complicated pattern but when left undisturbed for a longer time spirals tend to cover the whole surface. They appear then clearly as double spirals presumably formed by a singular line (Fig. 21). The beat-like structures still persist but in their centers spirals may also have developed (Fig. 22).

12. Focal Conics and Fan Texture Variations of Cholesterics

It is possible to obtain textures for which the twist axis remains more or less in the plane of the film and consequently, since $\mathbf{t} \cdot \operatorname{curl} \mathbf{t} = 0$, has a constant orientation along the verticals through the film. These textures are usually classified as fan textures because of a similarity with smectic fan textures.

A texture resembling a focal conic texture of smectic phases can also be obtained sometimes together with the fan texture in the same sample. Figure 23 shows such a " focal conic " texture with a surface pattern similar to that of Fig. 21. Presumably the pattern consists also of spirals which are, however, not clearly recognizable here. This texture is optically active which indicates that the twist axis in inner parts of the sample turns normal to the film. The center part of the spirals is colored differently and marked by a somewhat blurred maltese cross. It is this feature together with the tendency to a hexagonal grouping that reminds of the pattern of certain smectic focal conic textures. But pairs of focal conic disclination lines which are characteristic for true focal conic textures are absent in the cholesteric textures. We will see that the cholesteric fan texture also does not have pairs of focal conic disclinations.

A typical fan texture in another part of the same sample is shown in Fig. 24. The texture is birefringent but not optically active which indicates that the twist field is in fact essentially parallel to the plane of the film. Such fan textures can act as diffraction gratings provided the periodicity of the twisted structure is larger than the wavelength of light ($p/2 > \lambda$). Intensive colors due to diffraction can

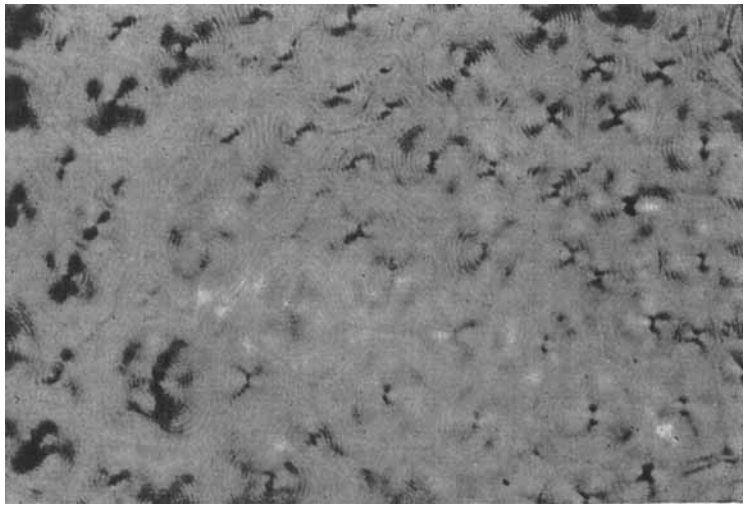

Figure 23. " Focal conic " texture. MBBA + 20% ChN between glass plates at 20 °C; focused on upper surface, crossed polarizers, approx. 440 × .

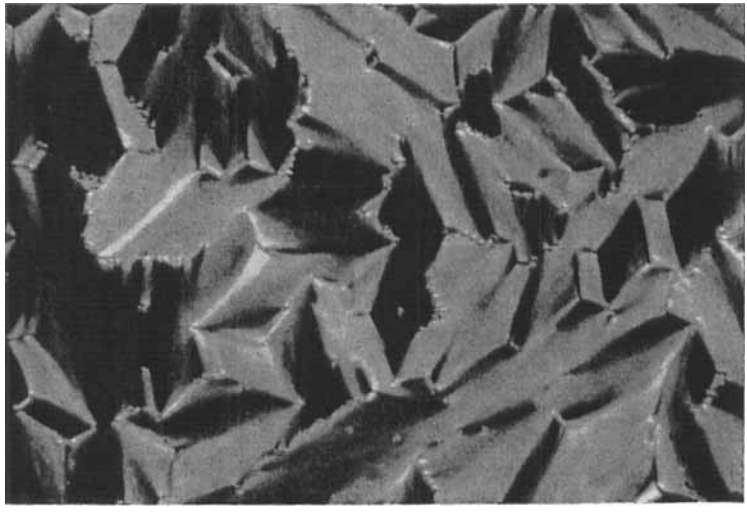

Figure 24. " Fan " texture. MBBA + 20% ChN between glass plates at 20 °C; focused on upper surface, crossed polarizers, approx. 440 × .

then be obtained. When $p/2 > \lambda$ it is possible in good (tempered) samples to recognize stripes (Fig. 25a and b). They indicate directly the quasi layered structure due to the twist. The stripes run normal to the twist field and their distance is equal to $p/2$.

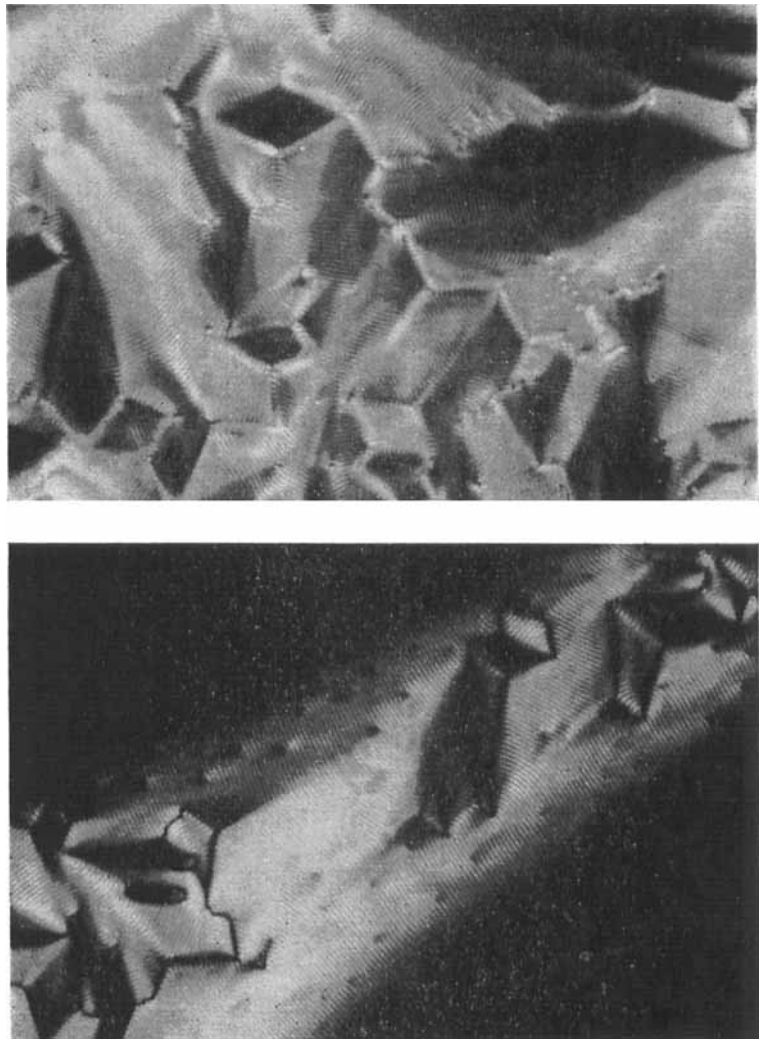

Figure 25. " Fan " texture. MBBA + 20% ChN, uncovered droplets at 20°C; focused on the surface, crossed polarizers, approx. 440 ×. Texture appears dark where polarization is parallel or perpendicular to stripes.

It can be recognized that the dominating structural features of these fan textures are vertical $+\frac{1}{2}$ and $-\frac{1}{2}$ lines in the field of the twist axis ($\lambda+$ and $\lambda-$ lines). They are the starting points for fairly sharp and often straightlined crests. The crests appear because the " layers " tend to form parallel planes which are bent only along certain edges where the orientation changes rather abruptly although still continuously.

In Fig. 25b a number of dark points can be seen. At each of these points an additional " layer " starts, or in other words a π-turn is added. They correspond accordingly to singular lines in the director-field which run vertical through the film.

13. Concluding Remarks

A useful qualitative understanding of the structure of disclinations in nematic liquid crystals has been reached. The disclinations can be classified by geometrical features. A main differentation may be made between singular and non-singular lines ($|s| = \frac{1}{2}$ and $|s| = 1$). They correspond to the full threads and half threads which have been discussed already by Lehmann. Singular points also occur and are in general positioned in the core of a non-singular line. The interactions between disclinations in nematics can be readily understood on the basis of the curvature elastic properties.

Cholesteric liquid crystals form the same basic types of disclinations as nematics but the general picture is much more complicated. The lines have a tendency to form bundles and do not merge and cancel as in nematics. Complicated networks of stable disclination lines form in this way and it may be questioned whether no other types of disclinations than the discussed ones contribute to it. Much remains unexplained on the special features of disclinations in cholesterics but initiated by the work of Kleman and Friedel good progress has been made in recent years.

An important area which is still unexplored is the dynamics of formation of disclinations and singularities. There will be different mechanisms for different types of disclinations. Non-singular lines may form gradually and grow with open ends, the half numbered lines must start as closed loops or originate on interfaces. Their formation will in general be connected with a rupture of the vectorfield.

Once the formation of disclinations is better understood it may open possibilities for new applications or allow improvements of existing devices. In addition it is of interest for possible biological functions of liquid crystals.

REFERENCES

1. Oseen, C. W., *Arkiv Matematik Astron. Fysik* A **19**, 1 (1925).
2. Oseen, C. W., *Fortschr. Chem. Phys. u. Phys. Chem.* **20**, 1 (1929).
3. Oseen, C. W., *Trans. Faraday Soc.* **29**, 883 (1933).
4. Oseen, C. W., *Arkiv Matematik Astron. Fysik* A **22**, 1 (1930).
5. Frank, F. C., *Disc. Faraday Soc.* **25**, 19 (1958).
6. Dzyalosh, I. E., *Sov. Phys. JETP* **31**, 773 (1970).
7. Nehring, J. and Saupe, A., *J. Chem. Soc., Faraday Trans. II* **68**, 1 (1972).
8. Dafermos, C. M., *Quart. J. Mech. and Appl. Math.* **23**, 49 (1970).
9. Williams, C., Pieranski, P. and Cladis, P. E., *Phys. Rev. Letters* **29**, 90 (1972).
10. Meyer, R. B., *Philos. Mag.* **27**, 405 (1973).
11. Cladis, P. E., Kleman, M., Pieranski, P. and Williams, C., Lecture, Fourth International Liquid Crystal Conference, Kent, Ohio, 1972.
12. Barrat, P. J., Lecture, Fourth International Liquid Crystal Conference, Kent, Ohio, 1972.
13. Cladis, P. E. and Kleman, M., *J. Phys.* **33**, 591 (1972).
14. Rault, J., Thesis, Paris, 1972.
15. Rault, J., *Sol. State Comm.* **9**, 1965 (1971).
16. Rault, J., *J. Physique* **33**, 383 (1972).
17. Kleman, M. and Friedel, J., *J. Physique* **30**, C4-43 (1969).
18. Scheffer, T. J., *Phys. Rev.* A **5**, 1372 (1972).
19. Rault, J., *Mol. Cryst.* **16**, 143 (1972).
20. Bouligand, Y. and Kleman, M., *J. Physique* **31**, 1041 (1970).